Electronic Supplementary Material (ESI) for Journal of Materials Chemistry C.

Supplementary Information

Novel bismuth ferrite-based lead-free incipient piezoceramics with high electromechanical response

Xing Liu, Jiwei Zhai*, Bo Shen

Key laboratory of Advanced Civil Engineering Materials of Ministry of Education, Functional Materials Research Laboratory, School of Materials Science & Engineering, Tongji University, 4800 Caoan Road, Shanghai 201804, China

*Corresponding author:

E-mail address: apzhai@tongji.edu.cn (J. Zhai)

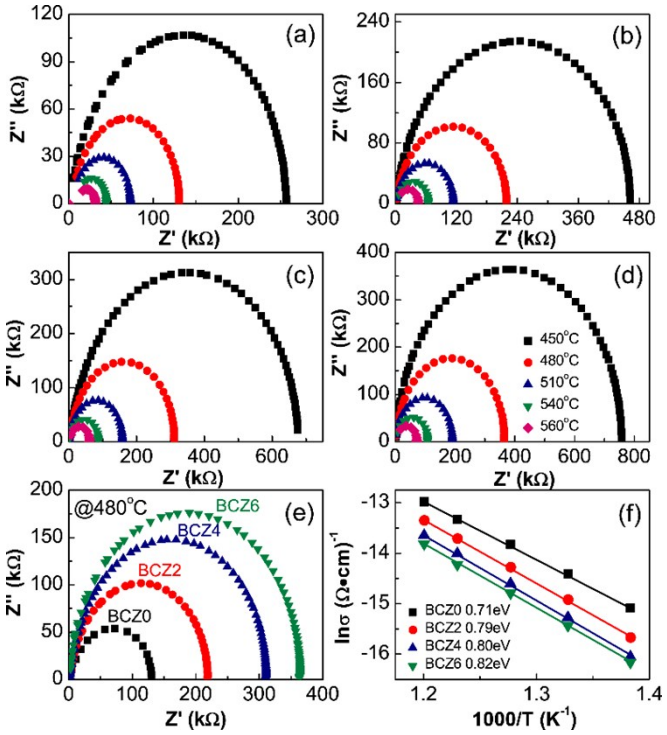

Fig. S1 The impedance spectra of (a) BCZ0, (b) BCZ2, (c) BCZ4 and (d) BCZ6 samples. (e) Comparison of the impedance spectra measured at 480 °C for different compositions. (f) lnσ *vs*. 1000/*T* plots for BCZ0-BCZ6 samples (symbol: experimental data, solid lines: linear fitting).

Fig. S1(a)-(d) provide the high-temperature impedance spectra of BCZ0-BCZ6 samples to explore their defect chemistry. Fig. S1(e) compares the impedance spectra of all compositions at 480 °C, and it is clear that the addition of BCZ gradually improves the impedance values. In addition, we further fitted the high-temperature conductivity using the Arrhenius law: $\sigma=\sigma_0\exp(-E_a/k_BT)$, where σ_0 is a constant, k is the Boltzmann constant and E_a is the activation energy.[1,2] The conductivity can be calculated by the equation: $\sigma=l/RS$, where R is the extrapolated intercept of the real-part impedance (Z'), l and S are thickness and cross-section area of ceramic samples, respectively. The plots of lnσ *vs*. 1000/*T* and linear fitting are presented in Fig. S1(f). The E_a values of BCZ0-BCZ6 samples are 0.71, 0.79, 0.80 and 0.82 eV, respectively, which are close to the activation energy of oxygen vacancies (E_a~1 eV), suggesting that the present system exhibits intrinsic electronic conduction and the oxygen vacancies may dominate the high-temperature conduction mechanism.[1,2] Moreover, the increase of E_a values with increasing BCZ content can be attributed to the reduced oxygen vacancy concentration, indicating that the current dopant would benefit to the improvement of electric insulation.[1,2]

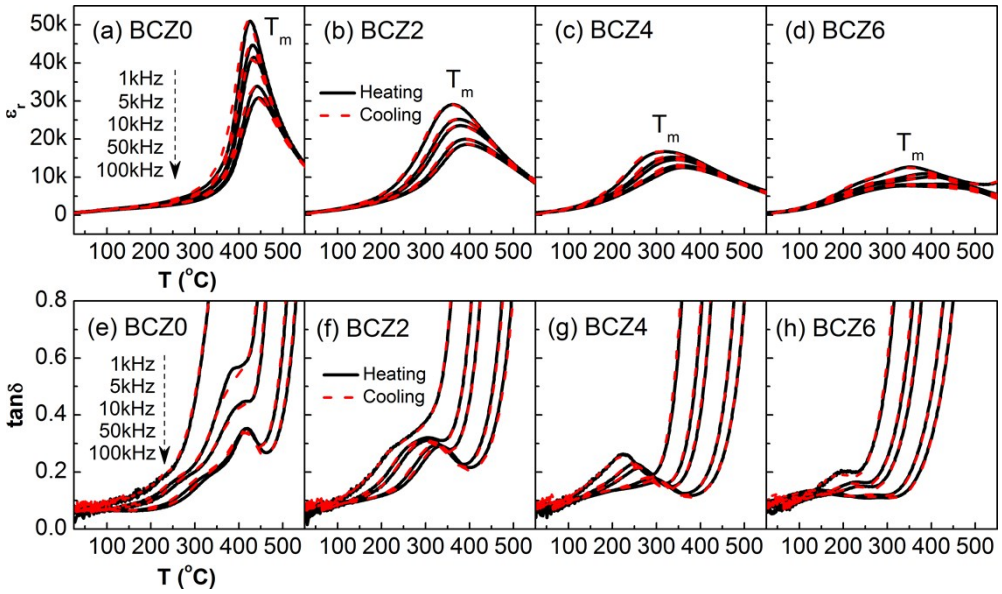

Fig. S2 Temperature dependent (a)-(d) dielectric constant (ε_r) and (e)-(h) loss tangent (tanδ) for BCZ0, BCZ2, BCZ4 and BCZ6 samples during heating and cooling processes.

Fig. S2(a)-(d) and (e)-(h) show the temperature dependent dielectric constant (ε_r) and loss tangent (tanδ) curves of BCZ0-BCZ6 samples measured at the frequencies of 1, 5, 10, 50 and 100 kHz. The heating and cooling rate was set as 2 °C /min. It is worth noting that almost no hysteresis can be observed during heating and cooling processes, implying that the thermal evolution possesses the characteristics of second-order phase transition.[3] All the samples display a dielectric peak at T_m (the temperature of dielectric maxima). With the increase of frequency, the dielectric constant decreases, the peaks at T_m on ε_r-T and tanδ-T curves shifts to the higher temperature side, corresponding to the relaxor like characteristics.[4] As shown in Fig. S2(a)-(d), the sharpness of dielectric peaks near T_m gradually decreases with increasing BCZ content, suggesting that the studied compositions become more and more diffuse.[4]

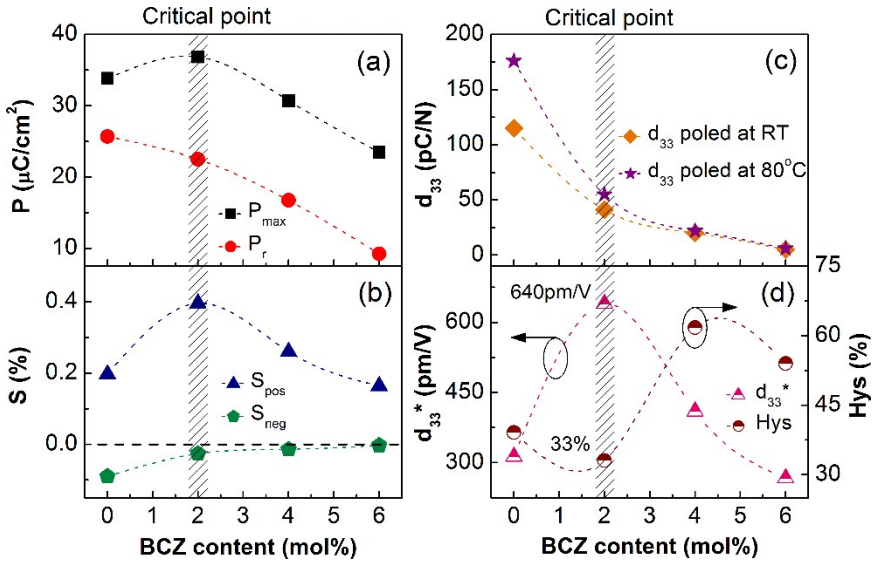

Fig. S3 (a) The maximum polarization (P_{max}) and remanent polarization (P_r), (b) positive strain (S_{pos}) and negative strain (S_{neg}), (c) d_{33} values at different poling temperatures, (d) d_{33}^* and hysteresis values with varying the BCZ content. The polarization and strain parameters were obtained at a frequency of 10 Hz.

Fig. S3 summarizes the maximum polarization (P_{max}) and remanent polarization (P_r), positive strain (S_{pos}) and negative strain (S_{neg}), d_{33} values at different poling temperatures, d_{33}^* and *Hys* values of all compositions. It can be seen that a slight addition of BCZ considerably disrupts the long-range polar order featured by the reduction of S_{neg}, P_r and d_{33} values.[5] The S_{pos}, d_{33}^* and *Hys* values of BCZ2 critical composition reach 0.4 %, 640 pm/V and 33 %, respectively, which is one of the best comprehensive strain performances among the Bi-based lead-free incipient ceramics.[6-16] The large strain property of BCZ2 can be attributed to a field-induced reversible relaxor-ferroelectric phase transformation.[5] With more addition of BCZ, the polarization and strain parameters gradually decrease, which is due to the increased relaxor phase content. Furthermore, as shown in Fig. S3(c), BCZ0 and BCZ2 samples display the higher d_{33} values at a high poling temperature of 80 °C compared to the d_{33} values poled at RT. This clearly implies the thermally activated poling process in BF-based ceramics. However, the improvement degree continuously decreases with more BCZ substitution, which is due to the enhanced relaxor dynamics.[5]

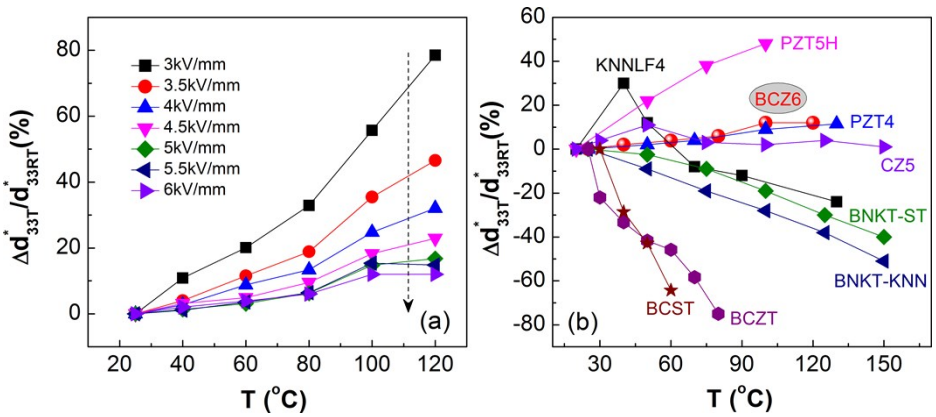

Fig. S4 (a) Normalized d_{33}^* values ($\Delta d_{33T}^*/d_{33RT}^*$) with varying the external field and temperature, the frequency was fixed at 10 Hz. (b) The variation rate $\Delta d_{33T}^*/d_{33RT}^*$ of BCZ2 sample at elevated temperatures and several actuator materials for comparison.[18-24]

Fig. S4(a) shows the normalized d_{33}^* values ($\Delta d_{33T}^*/d_{33RT}^*$) of BCZ2 sample as a function of external field and temperature. It can be seen that the d_{33}^* values tend to be more stable with increasing temperature at a higher external field. The large poling field can effectively force the oriented growth of PNRs in non-polar matrix since the high field can overcome the random field effects.[17] As a result, the transformation from ergodic relaxors to long-range ferroelectric phase becomes more complete, which can benefit the temperature stability of electrostrains.[17] Fig. S4(b) compares the variation rate $\Delta d_{33T}^*/d_{33RT}^*$ values of PZT-, $BaTiO_3$ (BT)-, (K, Na)NbO_3 (KNN)- and NBT-based ceramics.[18-24] The variation of d_{33}^* values keeps within 12 % up to 120 °C. It is found that the thermal stability of strain performance of BCZ2 composition is superior to the commercial PZT, BT-based ((Ba, Ca)(Zr, Ti)O_3/BCZT, (Ba, Ca)(Sn, Ti)O_3/BCST) ceramics and many other NBT-based ceramics.[18-24] Although the KNN-based CZ5 ceramics exhibit excellent thermal endurance, the current BCZ2 sample possesses two times larger d_{33}^* value than that of CZ5 ceramics (d_{33}^*=325 pm/V for CZ5, d_{33}^*=640 for BCZ2).[20] These results indicate that the current BCZ2 composition presents promising potentials in actuator applications requiring high strain output as well as the temperature stability.

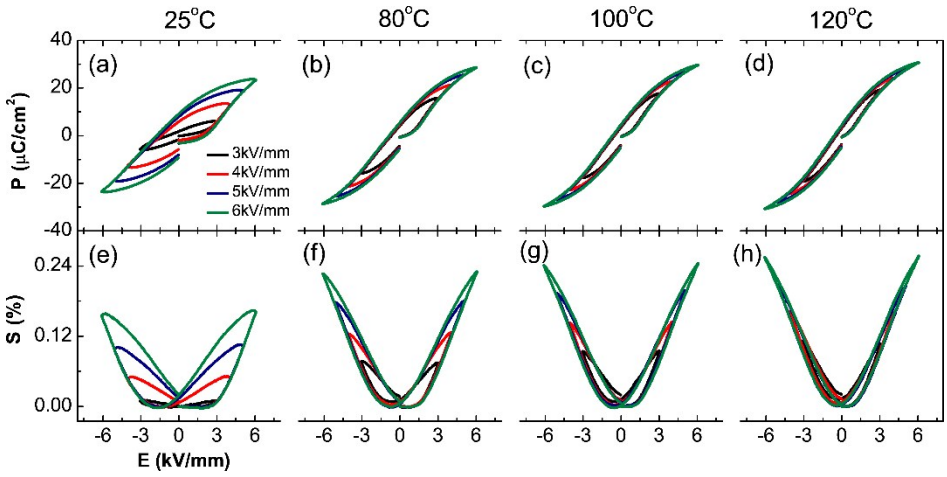

Fig. S5 (a)-(d) *P-E* hysteresis loops and (e)-(h) strain curves of BCZ6 sample measured at different electric fields and temperatures, the frequency was fixed at 10 Hz.

Fig. S5 shows the *P-E* hysteresis loops and strain curves of BCZ6 sample measured at different electric fields and temperatures. It can be seen that the polarization and strain loops become more saturated with increasing poling field since a higher external field can provide more driving force for microdomain switching.[17] With increasing temperature, the polarization and strain curves tend to be slimmer along with the steep reduction in hysteresis. This is due to the fact that the size of PNRs will decrease while their dynamics enhance at high temperatures, i.e., the relaxor degree strengthens continuously with increasing temperature, leading to the reduction of hysteresis effects.[25]

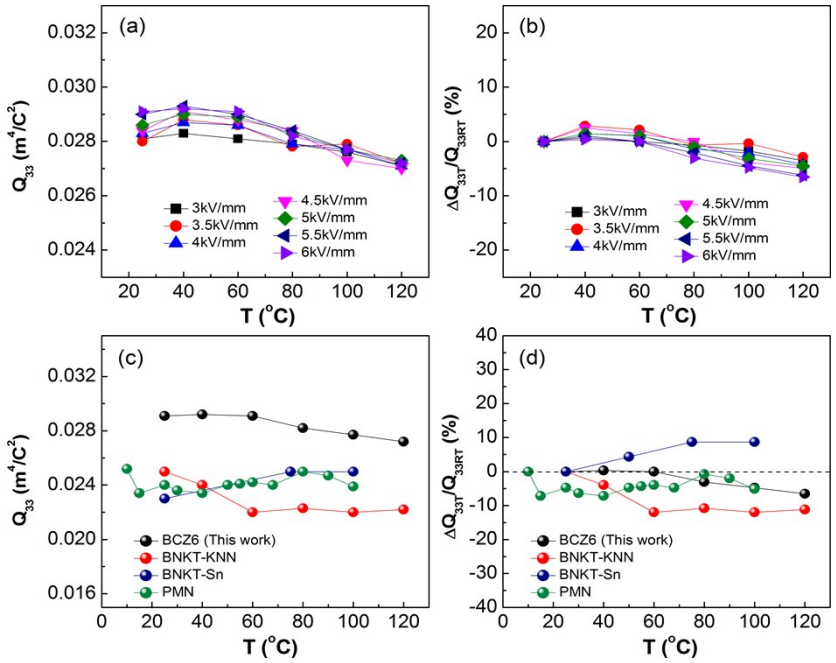

Fig. S6 (a) Q_{33} values and (b) the corresponding variation rate $\Delta Q_{33T}/Q_{33RT}$ of BCZ6 sample measured at different electric fields and temperatures, the frequency was fixed at 10 Hz; (c) Thermal stability of Q_{33} values and (d) the variation rate $\Delta Q_{33T}/Q_{33RT}$ of BCZ6 sample (at 6 kV/mm and 10 Hz) and several representative electrostrictive systems.[27-29]

Fig. S6(a) shows the Q_{33} values of BCZ6 sample as a function of electric field and temperature. The corresponding variation rate $\Delta Q_{33T}/Q_{33RT}$ was shown in Fig. S6(b). It is clear that the Q_{33} values of BCZ6 composition present a weak dependence of external field and temperature since the electrostriction is an intrinsic effect in piezoelectrics.[26] The variation rate $\Delta Q_{33T}/Q_{33RT}$ keeps less than 6.5 % in a wide temperature range of RT-120 °C, indicating that BCZ6 composition is a promising electrostrictor material in high-precision positioning devices. Fig. S6(c) shows the temperature dependence of Q_{33} values of BCZ6 sample (at 6 kV/mm and 10 Hz) and several representative electrostrictive systems for comparison,[27-29] and the variation rate $\Delta Q_{33T}/Q_{33RT}$ was shown in Fig. S6(d). It can be seen that the thermal stability of electrostrictive property for BCZ6 sample is comparable to other NBT-based and lead-based electrostrictive systems.[27-29]

References

1 F. Yang, M. Li, L. Li, P. Wu, E. P. Velázquez and D. C. Sinclair, *J. Mater. Chem. A*, 2018, **6**, 5243.

2 M. Li, M. J. Pietrowski, R. A. D. Souza, H. Zhang, I. M. Reaney, S. N. Cook, J. A. Kilner and D.C. Sinclair, *Nat. Mater.*, 2013, **13**, 31.

3 W. Jo, J. Daniels, D. Damjanovic, W. Kleemann and J. Rödel, *Appl. Phys. Lett.*, 2013, **102**, 192903.

4 A. A. Bokov and Z. G. Ye, *J. Mater. Sci.*, 2006, **41**, 31.

5 W. Jo, T. Granzow, E. Aulbach, J. Rödel and D. Damjanovic, *J. Appl. Phys.*, 2009, **105**, 094102.

6 J. Hao, W. Li, J. Zhai and H. Chen, *Mat. Sci. Eng. R*, 2019, **135**, 1.

7 W. Jo, R. Dittmer, M. Acosta, J. Zang, C. Groh, E. Sapper, K. Wang and J. Rödel, *J. Electroceram.*, 2012, **29**, 71.

8 S. T. Zhang, A. B. Kounga, E. Aulbach, H. Ehrenberg and J. Rödel, *Appl. Phys. Lett.*, 2007, **91**, 112906.

9 M. H. Lee, D. J. Kim, J. S. Park, S. W. Kim, T. K. Song, M. H. Kim, W. J. Kim, D. Do and I. K. Jeong, *Adv. Mater.*, 2015, **27**, 6976.

10 S. O. Leontsev and R. E. Eitel, *J. Am. Ceram. Soc.*, 2009, **92**, 2957.

11 L. F. Zhu, B. P. Zhang, J. Q. Duan, B. W. Xun, N. Wang, Y. C. Tang and G. L. Zhao, *J. Eur. Ceram. Soc.*, 2018, **38**, 3463.

12 G. H. Ryu, A. Hussain, M. H. Lee, R. A. Malik, T. K. Song, W. J. Kim and M. H. Kim, *J. Eur. Ceram. Soc.*, 2018, **38**, 4414.

13 R. A. Malik, A. Zaman, A. Hussain, A. Maqbool, T. K. Song, W. J. Kim, Y. S. Sung and M. H. Kim, *J. Eur. Ceram. Soc.*, 2018, **38**, 2259.

14 T. Zheng, C. Zhao, J. Wu, K. Wang and J. F. Li, *Scripta Mater.*, 2018, **155**, 11.

15 D. Wang, A. Khesro, S. Murakami, A. Feteira, Q. Zhao and I. M. Reaney, *J. Eur. Ceram. Soc.*, 2017, **37**, 1857.

16 D. Zheng and R. Zuo, *J. Am. Ceram. Soc.*, 2015, **98**, 3670.

17 D. Maurya, A. Pramanick, M. Feygenson, J. C. Neuefeind, R. J. Bodnar and S. Priya, *J. Mater. Chem. C*, 2014, **2**, 8423.

18 D. Wang, Y. Fotinich and G. P. Carman, *J. Appl. Phys.*, 1998, **83**, 5342.

19 Y. Saito, H. Takao, T. Tani, T. Nonoyama, K. Takatori, T. Homma, T. Nagaya and M. Nakamura, *Nature*, 2004, **432**, 84.

20 K. Wang, F. Z. Yao, W. Jo, D. Gobeljic, V. V. Shvartsman, D. C. Lupascu, J. F. Li and J.

Rödel, *Adv. Funct. Mater.*, 2013, **23**, 4079.

21 K. Wang, A. Hussain, W. Jo and J. Rödel, *J. Am. Ceram. Soc.*, 2012, **95**, 2241.

22 S. T. Zhang, A. B. Kounga, E. Aulbach, W. Jo, T. Granzow, H. Ehrenberg and J. Rödel, *J. Appl. Phys.*, 2008, **103**, 034108.

23 L. F. Zhu, B. P. Zhang, L. Zhao and J. F. Li, *J. Mater. Chem. C*, 2014, **2**, 4764.

24 J. Hao, W. Bai, W. Li and J. Zhai, *J. Am. Ceram. Soc.*, 2012, **95**, 1998.

25 X. Liu, J. Zhai, B. Shen, F. Li, Y. Zhang, P. Li and B. Liu, *J. Eur. Ceram. Soc.*, 2017, **37**, 1437.

26 F. Li, Z. Xu and S. Zhang, *Appl. Phys. Rev.*, 2014, **1**, 011103.

27 J. Hao, Z. Xu, R. Chu, W. Li and J. Du, *J. Mater. Sci.*, 2015, **50**, 5328.

28 H. S. Han, W. Jo, J. K. Kang, C. W. Ahn, I. W. Kim, K. K. Ahn and J. S. Lee, *J. App. Phys.*, 2013, **113**, 154102.

29 K. Uchino, S. Nomura, L. E. Cross, R. Newnham and S. Jang, *J. Mater. Sci.*, 1981, **16**, 569.